Enlarged sheet of $ZnS(en)_{0.5}$ Hybrid Semiconductors with photocatalytic activity

Agileo Hernández-Gordillo, Etel Maya-Flores, Vicente Rodríguez-Gonzalez

PII: S0167-577X(15)00244-X
DOI: http://dx.doi.org/10.1016/j.matlet.2015.02.051
Reference: MLBLUE18506

To appear in: *Materials Letters*

Received date: 3 January 2015
Accepted date: 10 February 2015

Cite this article as: Agileo Hernández-Gordillo, Etel Maya-Flores, Vicente Rodríguez-Gonzalez, Enlarged sheet of $ZnS(en)_{0.5}$ Hybrid Semiconductors with photocatalytic activity, *Materials Letters,* http://dx.doi.org/10.1016/j.matlet.2015.02.051

Enlarged Sheet of ZnS(en)$_{0.5}$ Hybrid Semiconductors with Photocatalytic Activity

Agileo Hernández-Gordillo[1a]*, Etel Maya-Flores[2], Vicente Rodríguez-Gonzalez[3]

[1]Instituto de Investigaciones en Materiales, Universidad Nacional Autónoma de México. Circuito Exterior SN, Ciudad Universitaria, CP 04510, México D.F., Coyoacán, México. Phone: +52 56224633. [a] Cátedras-Conacyt.

[2]Instituto Mexicano del Petróleo, Eje central Lázaro Cárdenas No.152, 07730 México, D.F., México.

[3]División de Materiales Avanzados, Instituto Potosino de Investigación Científica y Tecnológica, Camino a la Presa San José 2055 Col. Lomas 4a. sección C.P. 78216, San Luis Potosí, S.L.P., México. *E-mail: *agileo12@hotmail.com, agileohg@iim.unam.mx.*

Abstract

Sheets of ZnS(en)$_{0.5}$ hybrid semiconductors were prepared by the precipitation method in an ethylenediamine-water solution and it was enlarged by varying the aging at a long period time. The characterization of the hybrid material was carried out by different techniques such as FTIR, DRS-UV-Vis spectroscopies and scanning electron microscopy (SEM). The number of intercalated ZnS layers in a ZnS(en)$_{0.5}$ hybrid semiconductor was proposed to be determined by XRD. The photocatalytic activity of the enlarged sheet of ZnS(en)$_{0.5}$ hybrid was investigated in the photoreduction of *4-nitrophenol* to *4-aminophenol* in the presence of hydrazine under UV light irradiation. The intrinsic photocatalytic activity of the ZnS(en)$_{0.5}$ semiconductor sheets was associated with the number of intercalated ZnS layers, and possible mechanism of the electron transfer process was discussed.

Keywords: Enlarged Sheets, ZnS(en)$_{0.5}$ Hybrid, Intercalated layers, 4-nitrophenol photoreduction.

INTRODUCTION

Zinc sulfide (ZnS) is a direct-gap semiconductor (3.2 eV) with interesting optical, electronic, physical, chemical and fluorescence properties and has extensive applications in optical devices and in heterogeneous photocatalysis [1-3]. Moreover, when a diamine organic molecule is linked to ZnS surface, it forms an inorganic-organic hybrid semiconductor, which are interconnected or separated by the organic molecules via coordinative bonds, all of which are composed of single atomic layers (***L***) of nanocomponents. This hybrid represents a class of laminar structures of type [MQ(L)x], (where M=Zn; Q=S, L=diamine molecule and x=0.5 or 1 [4]. Due to that the diamine organic insulators act as spacers, it prevents the interactions among the neighboring layers nanocomponents and the electronic and optical properties are enhanced, exhibiting a large band gap energy value (4.1±0.1 eV) and high band-edge absorption that stems from a strong ZnS-layer-by-layer quantum-confinement effect. Typically, this hybrid semiconductor exhibits sheets morphology with different dimension [5-8].

The enhanced optical-electronic property provides the thermodynamic conditions (favorable negative position of the conduction band) to conduct photocatalytic redox reactions like the photooxidation reaction of diverse pollutant compounds such as acid fuchsine and methylene blue dyes [9-12]; however, applications in photoreduction reactions of heavy metal ions [13] and H_2 production [14] are scarce. Considering that the physical and chemical properties of semiconductors nanostructured strongly depend on their structures and shape sizes, a variety of materials nanostructured such as nanorods, nanotubes, and hollow nanostructures have been synthesized by using diverse methods, obtaining semiconductor materials with larger surface area and high photochemical activity [2].

Photoassisted reduction of nitroaromatic molecules (pollutant compounds) ranging from *4-nitrophenol* (*4-NP*) to *4-aminophenol* (*4-AP*) using UV light has been considered as one of the most important photocatalytic reactions because of the converted aminophenols, which are used as photographic developers, corrosion inhibitors, dyeing agents, etc., yield valuable amino reagents for chemical products used in diverse industries [15]. This photoassisted chemical reduction of *4-NP* has been explored by using semiconductors such doped Mn-ZnS [16], metals-TiO_2 [17-19], halloysite nanotube/Fe_3O_4 [20] and TiO_2-graphene [21] in the presence of $NaBH_4$ as hole scavengers. Recently we have shown the photoreduction of 4-nitrophenol by using AgNPs-TiO_2 [22], AgNPn-TiO_2-Cu [23] doped semiconductors in the presence of hydrazine as hole scavenger; however, the photocatalytic property of $ZnS(en)_{0.5}$ hybrid semiconductor has not been studied in this photoassisted reduction reaction.

$ZnS(en)_{0.5}$ hybrid semiconductors in sheet form were synthesized in an ethylenediamine-water solution by the precipitation method, varying the aging time from 6 to 72h. The formation of the hybrid was confirmed by different techniques such as XRD, FTIR, and DRS-UV-Vis spectroscopies, whereas the morphology of the formed sheets was determined by scanning electron microscopy (SEM). Particularly, the number of intercalated ZnS layers in the hybrid sample was determined by XRD. The photocatalytic property of the $ZnS(en)_{0.5}$ hybrid semiconductor was investigated through the photoassisted reduction of *4-nitrophenol* in the presence of hydrazine. The effects of the number of intercalated ZnS layers and the textural properties of the sheet semiconductors on the photochemical activity were considered.

METHODOLOGY

Hybrid $ZnS(en)_{0.5}$ semiconductors were prepared by the conventional precipitation method in an ethylenediamine aqueous solution at relatively low temperature, varying the aging time [14]. By a typical procedure, appropriate amounts of $Zn(NO_3)_2H_2O$ (Reasol) were first dissolved in an ethylenediamine-water solution (at 60 % vol. of *en*), and thiourea (Reasol) was immediately added (stoichiometry molar ratio S/Zn=3). Then, the homogeneous solution was heated at boiling point (~110°C) and refluxed at a desired aging time (6, 48 and 72h). The solid was recovered by filtration, washed with an ethanol-water solution and dried at 110°C in an oven all night long. The obtained products were labeled as **S-X*L***, where X represents a number of intercalated ZnS Layer*:* 13, 22 and 29*L*. The prepared semiconductors were characterized by X-ray powder diffraction using a BRUKER D2 PHASER diffractometer. The scanning rate was 0.01 °/S in the 2θ range from 7 to 60 degrees (2 theta). The number of intercalated ZnS layers (*N* layer) was estimated from the peak widths using the Scherrer equation: $D_{plates} = k\ 0.89/b\ cos\ h$, where D_{plates} is the average particle size of the platelet or sheet thickness, *k* is the X-ray wavelength (1.5404 Å) and *b* is the half-width of the peak at 10.4° of 2 theta (*h*). The UV-band-gap energy value (E_g) was estimated using the Kubelka-Munk method (see Suplementary Information, Figure ***S2***) from the absorption spectra obtained with a Varian Cary-100 spectrometer equipped with an integration sphere. The FTIR absorption spectra of the samples were obtained with a Shimadzu IR-440 FTIR spectrometer from 600 to 4000 cm^{-1} equipped with ATR accessory. The morphology of the sheets of the hybrid material was revealed by field emission scanning electron microscopy (FESEM) using a Helios NanoLab 600i. The photoassisted chemical reaction was performed in a glass-home-made reactor system containing 200 mL of an aqueous solution with

10 ppm of *4-NP* (Aldrich), 0.5 M of N_2H_4 (Aldrich) and 0.15 g/L of photocatalyst powder [22]. The suspension was maintained by magnetic stirring (600 RPM) at room temperature and left in the dark condition for 1h. After the adsorption-desorption equilibrium, the system was irradiated with UV light supplied by a high pressure Hg lamp emitting λ=254 nm, of 4400 μW/cm^2 encapsulated in a quartz tube which is immersed in the solution. The estimation of the *4-NP* concentration was made from UV-Vis spectroscopy using a Varian-Cary 5000 spectrometer by following the disappearance of the absorption band at 400 nm for *4-nitrophenolate* ions. The Langmuir-Hinshelwood kinetic model is usually applicable to describe the kinetics of *4-NP* reduction. So, kinetic data such as the apparent rate constant (K_{app}) in reduction reactions were obtained considering a pseudo zero order [22]. Additional photoassisted chemical reaction experiments were carried out with TiO_2-P25 used as reference photocatalyst under the same conditions.

RESULTS AND DISCUSION

The ZnS(en)$_{0.5}$ hybrid prepared at different aging times exhibited the typical sheet-like morphology [7-11] with different dimensions. At 6h of aging, the sample presents sheet with diameter of D=652 nm and length of L=1.28 μm dimensions (Figure 1a) with lower thickness than those obtained at long aging times, which in the case of the samples obtained at 48 and 72h, whose dimensions were enlarged to D=120-150 nm and L=606-687nm (Figure 1b and 1c). The sample prepared at 48h exhibits square edges, but when the aging time was extended at 72h, the edges evolve to an oval form. The X-ray diffraction patterns for all samples (Figure 2a) can be indexed as orthorhombic structures of the typical ZnS(en)$_{0.5}$ hybrid material with good crystallization, and the reflection peaks at 29.4 and 53.20° seem to be the principal planes of the orthorhombic structure [11], [24]. All the sheet samples exhibit an additional reflection peak at

low angle (10.2°), which is characteristic of a material with intercalated layer structures (typical of superstructures), caused by the presence of the organic amine molecule between the two ZnS layers [3], [10]. The calculated interplanar distance (d_{layer}=0.86 nm) corresponds to the distance of the structure ZnS layers separated by the confined ethylenediamine (*en*) [25]. From this reflection peak, the platelet or sheet thickness (D_{plates}), determined by the Debye-Sherrer equation, could be associated with the number of intercalated ZnS layers (*N Layer*), which is increased from 13 to 29 ZnS layers as the aging time is also increased. This fact indicates that the **S-29*L*** sample is densely packed forming a multilayer stacked structure [26]. The FTIR spectra for the sheet of the ZnS(en)$_{0.5}$ hybrid exhibits stretching vibrations at 3240 (1st), 2866 (2nd), and 1140 cm^{-1} peaks (3rd dashed line, Figure ***S1***) assigned to the –NH_2, –CH_2, and C–N stretching vibration bands, respectively, which are indicative of the ZnS*(en)*$_{0.5}$ complex formation [13], where the ethylenediamine organic molecule is confined between two ZnS layers.

The UV-Vis diffuse reflectance spectra for all the ZnS(en)$_{0.5}$ hybrid (Figure 2b) exhibit a sharp absorption edge at 252 nm (dashed line), indicating the UV-C electronic transition stemming from the hybrid metal-ligand complex [26] or the quantum confinement effect of the stacked layers [3]; however, for the **S-29*L*** sample, two additional absorption edges at 290 and 368 nm (dashed line) were detected. The fundamental absorption edge could be related to electronic transitions of the hybrid complex and the second one could probably be caused by surface defects [27]. The UV-band-gap energy value for all the ZnS(en)$_{0.5}$ hybrid semiconductor sheets is 4.5+1eV (Table 1 and Figure ***S2***), which indicates a strong quantum confinement effect [7]. This result suggests that the optical-electronic properties of the ZnS(en)$_{0.5}$ hybrid semiconductors are affected as the aging time is increased due to the stacking multilayers of 29 Layers of ZnS. The N_2 physisorption confirms the laminar arrangement of the sheet samples, Figure 2c. The

nitrogen adsorption-desorption isotherms are type IV; according to the IUPAC classification, this characteristic isotherm corresponds to layered materials [28]. The isotherms present a hysteresis loop from 0.6 to 0.95 (H2 type), which represents a homogenous distribution of *en* molecules between over the layers in conjunction with the layered structure of ZnS(*en*) materials, which match to interlap voids. For the **S-13*L*** sample, the hysteresis at high relative pressure is broad, which is associated with pores in the structure layers, whereas the hysteresis for the **S-29*L*** sample is narrow because porosity is decreased when the ZnS layers are stacked. The specific surface area of the ZnS$(en)_{0.5}$ hybrid semiconductors were decreased from 55 to 30 m^2/g (Table 1) as the stacking of ZnS layers was increased.

The aqueous solution of *4-NP* in the presence of hydrazine shows the characteristic absorption band of the *4-nitrophenolate* (*4-NPate*) ion at 400 nm [22]. After the UV irradiation process, when the ZnS$(en)_{0.5}$ sheet photocatalyst was added, the absorption band of the *4-NPate* ion got reduced within 40 min and a new absorption band at 295-300 nm, characteristic of the *4-aminophenolate* (*4-APate*) formation [29], is built-up (Figure 3A). The presence of two isosbestic points at 280 and 313 nm is indicative of the photoconversion of *4-Nitrophenolate* to the *4-Aminophenolate* ion in equilibrium, indicating that secondary product is not formed [30]. The kinetic curve is adjusted to zero order (Figure *S3A*). The **S-29L** photocatalyst shows a high apparent zero rate constant value (1.6 Mh^{-1}), which is 11% higher than that of the **S-13*L*** photocatalyst, it was even 36% more active than the TiO_2-P25 used as a reference photocatalyst (1.17 Mh^{-1}, Figure ***S3B***). Considering that the specific surface area varies as a function of *N layers* of ZnS (Table 1), the intrinsic photocatalytic activity of the **S-29*L*** sample is 3.26 $Mh^{-1}m^{-2}$, despite the specific surface area is low (30 m^2/g), resulting in an activity increased 3.6 times higher than those featured by the **S-13*L*** photocatalysts. From these results, the photocatalytic

activity of the enlarged sheet is increased as the number of stacked ZnS layers is increased too, improving the electron transfer process [31]. Therefore, the stacking of the ZnS layers improving the contact of the *4-NPate* reactant with the ZnS surface to carry out the electron transfer process (Figure 3B). Thus the photoassisted chemical reduction of *4-nitrophenol* to *4-aminophenol* using enlarged sheet of ZnS$(en)_{0.5}$ hybrid semiconductor in the presence of hydrazine follows a similar, previously-reported mechanism [22], [23], where the photogenerated h^+ react with the hydrazine adsorbed on the surface to form the hydrazyl radical (NH_2NH^*) until to tetrazane formation [32], while the photogenerated e^- are transferred from the hybrid surface to the acceptor nitro-aromatic contaminant via the electron-transfer process.

CONCLUSIONS

Hybrid ZnS$(en)_{0.5}$ sheets with intercalated ZnS layers were obtained by the precipitation method, varying the aging time from 6 to 72h. Similar electronic-optical properties of all the sheets were obtained independently of the number of intercalated ZnS layers (13-29 layers), but the specific surface area was decreased as ZnS layers are stacked. High stacking of ZnS layers of the sheets improves the intrinsic photocatalytic activity, allowing the fast electron-transfer process to the pollutant molecule, achieving the reduction of *4-nitrophenol* in the presence of hydrazine under UV light irradiation.

Acknowledgements

We thank CONACYT for financial support through the SEP CONACYT-CB-2011/169597 project. Agileo Hernández-Gordillo thanks to CONACYT for financial support through the Cátedras-Conacyt/1169 project.

REFERENCES

[1]. Yang J., Peng J., Zou R., Peng F., Wang H., Yu H., Lee J., Mesoporous zinc-blende ZnS nanoparticles: synthesis, characterization and superior photocatalytic properties, Nanotech. 2008;19(25):255603-255609.

[2]. Zhao Z., Geng F., Cong H., Bai J., Cheng H.M., A simple solution route to controlled synthesis of ZnS submicrospheres, nanosheets and nanorods, Nanotech. 2006;17:4731–4735.

[3]. Kim Y., Jang D-J, Facile one-step hydrothermal fabrication of single-crystalline ZnS nanobelts with narrow band-edge luminescence, RSC Advances, 2013;3:16945.

[4]. Huang X. Li J., From Single to Multiple Atomic Layers: A Unique Approach to the Systematic Tuning of Structures and Properties of Inorganic-Organic Hybrid Nanostructured Semiconductors, J. Am. Chem. Soc. 2007;129:3157-3162.

[5]. Kim Y., Kim J-Y, Jang D-J, One-Pot and Template-Free Fabrication of ZnS(ethylenediamine)$_{0.5}$ Hybrid Nanobelts, J. Phys. Chem. C 2012;116:10296-10302.

[6]. Yu S.H., Yang J., Qian Y.T., Yoshimura M., Optical properties of ZnS nanosheets, ZnO dendrites, and their lamellar precursor ZnS (NH2CH2CH2NH2)0.5, Chem. Phys. Letters 2002;361:362–366.

[7]. Yu S.H., Yoshimura M., Shape and Phase Control of ZnS Nanocrystals: Template Fabrication of Wurtzite ZnS Single-Crystal Nanosheets and ZnO Flake-like Dendrites from a Lamellar Molecular Precursor ZnS($NH_2CH_2CH_2NH_2$)$_{0.5}$, Adv. Mater. 2002;14(4): 296-300.

[8]. Mosca R., Ferro P., Calestani D., Nasi L., Besagni T., Licci F., Solvothermal synthesis of ZnS[$C_2H_4(NH_2)_2$]$_{0.5}$ nanosheets, Cryst. Res. Technol. 2011; 46(8):818–822.

[9]. Dai J., Jiang Z., Li W., Bian G., Zhu Q., Solvothermal preparation of inorganic–organic hybrid compound of [$(ZnS)_2$(en)] and its application in photocatalytic degradation, Mater. Lett. 2002;55:383– 387.

[10]. Nasi L., Calestani D., Besagni T., Ferro P., Fabbri F., Licci F., Mosca R., ZnS and ZnO Nanosheets from $ZnS(en)_{0.5}$ Precursor: Nanoscale Structure and Photocatalytic Properties, J. Phys. Chem. C 2012;116:6960−6965.

[11]. Kole A.K., Tiwary C.S., Kumbhakar P., Ethylenediamine assisted synthesis of wurtzite zinc sulphide nanosheets and porous zinc oxide nanostructures: near white light photoluminescence emission and photocatalytic activity under visible light irradiation, CrystEngComm. 2013;15:5515–5525.

[12]. Xi G., Wang C., Wang X., Zhang Q., Xiao H., From ZnS-en0.5 Nanosheets to Wurtzite ZnS Nanorods under Solvothermal Conditions, J. Phys. Chem. C 2008;112:1946-1952.

[13]. Hernández-Gordillo A., Tzompantzi F., Gómez R., Enhanced photoreduction of Cr(VI) using $ZnS(en)_{0.5}$ hybrid semiconductor,Catal. Comm. 2012;19:51–55.

[14]. Hernández-Gordillo A., Tzompantzi F., Gómez R., An efficient ZnS-UV photocatalysts generated in situ from $ZnS(en)_{0.5}$ hybrid during the H_2 production in methanol-water solution, Int. J. Hydrogen Energy 2012;37:17002-17008.

[15]. Panigrahi S., Basu S., Praharaj S., Pande S., Jana S., Pal A., Ghosh S.K., Pal T., Synthesis and Size-Selective Catalysis by Supported Gold Nanoparticles: Study on Heterogeneous and Homogeneous Catalytic Process, J. Phys. Chem. C 2007;111:4596-4605.

[16]. Sarkar S., Guria A.K., Pradhan N., Influence of doping on semiconductor nanocrystals mediated charge transfer and photocatalytic organic reaction, Chem. Commun. 2013;49:6018-6020.

[17]. Shiraishi Y., Togawa Y., Tsukamoto D., Tanaka S., Hirai T., Highly Efficient and Selective Hydrogenation of Nitroaromatics on Photoactivated Rutile Titanium Dioxide, ACS Catal. 2012;2:2475−2481.

[18]. Mohamed M., Al-Sharif M.S., Visible light assisted reduction of 4-nitrophenol to 4-aminophenol on Ag/TiO_2 photocatalysts synthesized by hybrid templates, Appl. Catal. B: Environm. 2013;142–143:432– 441.

[19]. Muniz-Miranda M., SERS monitoring of the catalytic reduction of 4-nitrophenol on Ag-doped titania nanoparticles, Appl. Catal. B: Environm. 2014;146:147–150.

[20]. Mu B., Wang W., Zhang J., Wang A., Superparamagnetic sandwich structured silver/halloysite nanotube/Fe_3O_4 nanocomposites for 4-nitrophenol reduction, RSC Adv., 2014;4:39439-39445.

[21]. Chao X., Yao Y., Rusheng Y., Xianzhi F., Enhanced photocatalytic performances of TiO_2-graphene hybrids on nitro-aromatics reduction to amino-aromatics, RSC Adv. 2013;3:18002-18008.

[22]. Hernández-Gordillo A., Arroyo M., Zanella R., Rodríguez-González V., Photoconversion of 4-nitrophenol in the presence of hydrazine with AgNPs-TiO_2 nanoparticles prepared by the sol‑gel method, J. Hazard. Mater. 2014;268:84-91.

[23]. Hernández-Gordillo A., Rodríguez-González V., Silver nanoparticles loaded on Cu-doped TiO_2 for the effective reduction of nitro-aromatic contaminants, Chem. Engin. J. 2015;261:53-59.

[24]. Ouyan X., Tsai T.Y., Chen D.H., Huang Q.J., Cheng W.H., Clearfield A., Ab initio structure study from in-house powder diffraction of a novel $ZnS(EN)_{0.5}$ structure with layered wurtzite ZnS fragment, Chem. Comm., 2003;7:886–887.

[25]. Sperinck S., Becker T., Wright K., Richmond W., Synthesis and characterisation of lamellar ZnS nanosheets containing intercalated diamines, J. Incl. Phenom. Macrocycl. Chem., 2009;65:89–95.

[26]. Zhao J., Yin J., Yang M., Controlled synthesis, conversion and photoluminescence properties of hierarchical flower-like $ZnS(En)_{0.5}$ superstructures, ZnS and ZnO, J. Alloys Compounds 2013;579:45–49.

[27]. Jang J.S., Yu C.J., Choi S.H., Ji S.M., Kim E.S., Lee J.S., Topotactic synthesis of mesoporous ZnS and ZnO nanoplates and their photocatalytic activity, J. Catal. 2008;254:144-155.

[28]. Condon J.B., "Surface area and porosity determinations by physisorption: measurements and theory" 2006 Elsevier, Amsterdam.

[29]. Tang M., Huang G., Zhang S., Liu Y., Li X., Wang X., Pang X., Qiu H., Low-cost removal of organic pollutants with nickel nanoparticle loaded ordered macroporous hydrogel as high performance catalyst, Mater. Chem. Phys. 2014;145:418-424.

[30]. Wunder S., Polzer F., Lu Y., Mei Y., Ballauff M., Kinetic Analysis of Catalytic Reduction of 4-Nitrophenol by Metallic Nanoparticles Immobilized in Spherical Polyelectrolyte Brushes, J. Phys. Chem. C 2010;114:8814-8820.

[31]. Chen F., Cao Y., Jia D., A facile route for the synthesis of ZnS rods with excellent photocatalytic activity, Chem. Engin. J. 2013;234:223–231.

[32]. Abe T., Taira N., Tanno Y., Kikuchi Y., Nagai K., Decomposition of hydrazine by an organic fullerene–phthalocyanine p–n bilayer photocatalysis system over the entire visible-light region, Chem. Commun. 2014;50:1950-1952.

Figures Captions

Figure 1. SEM images for the sheets of ZnS(en)$_{0.5}$ hybrid semiconductors prepared at different aging times: b) 6h (sheet), c) 48 (enlarged sheet) and c) 72h (enlarged sheet).

Figure 2. A) X-ray diffraction patterns, B) UV-Vis diffuse reflectance spectra and C) N_2 adsorption-desorption isotherms for the ZnS(en)$_{0.5}$ hybrid semiconductors prepared at different aging times; 6h (S-13*L*), 48h (S-22*L*) and 72h (S-29*L*).

Figure 3. A) UV-Vis spectra, B) Schematic representation of the mechanism of the photoconversion of *4-nitrophenol* to *4-aminophenol* in the presence of hydrazine over the stacked layer structure of the enlarged sheets of ZnS(en)$_{0.5}$ hybrid semiconductor.

Tables Captions

Table 1. Data of the *N layer*, specific surface area, band-gap energy, apparent rate constant and photocatalytic activity intrinsic for the sheets ZnS(en)$_{0.5}$ semiconductors.

Table 1. Data of the *N layer*, specific surface area, band-gap energy, apparent rate constant and photocatalytic activity intrinsic for the sheets $ZnS(en)_{0.5}$ semiconductors.

Sample	*N* Layer	E_g (eV)	S_g (m^2/g)	k_{app} ($M\ h^{-1}$)	k_{Int} ($M\ h^{-1}m^{-2}$)
S-13*L*	~13	4.5	55	1.44	0.87
S-22*L*	~22	4.6	43	1.35	1.50
S-29*L*	~29	4.5 (3.9)*	30	1.60	3.26

N Layer= Numbers of intercalated layers, E_g= Band-gap energy, *Second band-gap, S_g= Specific surface area, k_{app}= Apparent zero rate constant, k_{Int}= Intrisic Activity

Highlights

- Enlarged sheet of hybrid ZnS(*en*)$_{0.5}$ semiconductors were obtained.
- High stacking of ZnS layers were acheieved at long aging time.
- Optical-electronic properties are similar at different intercalated ZnS layers.
- High activity in 4-NPate reduction was achieved with ZnS(*en*)$_{0.5}$ and hydrazine.

Graphical Abstract

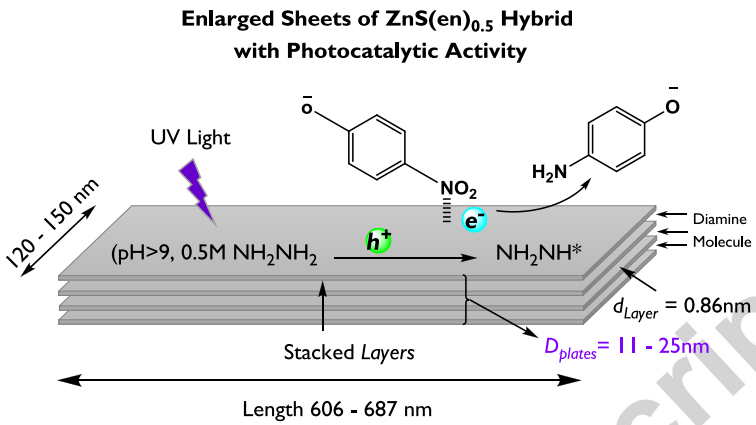

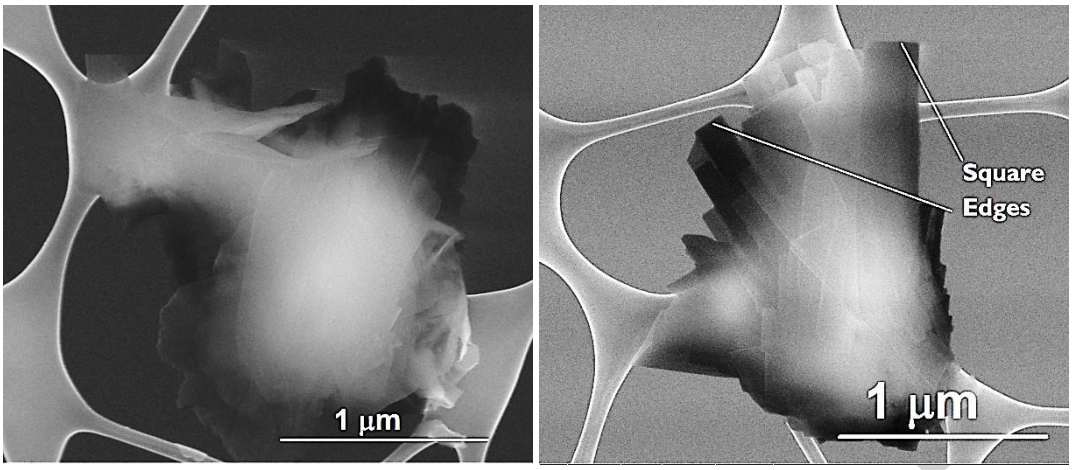

a) b)

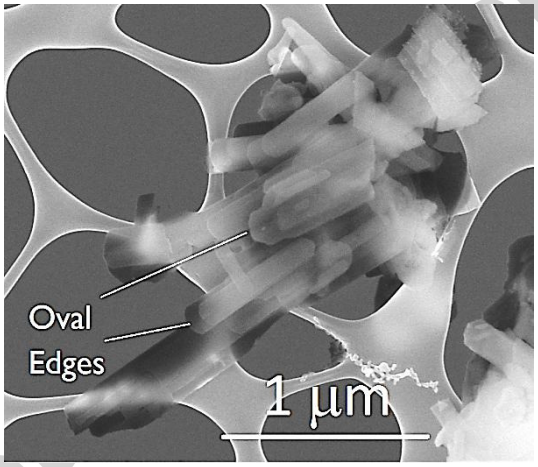

c)

Figure 1. SEM images for the sheets of $ZnS(en)_{0.5}$ hybrid semiconductors prepared at different aging times: b) 6h (sheet), c) 48 (enlarged sheet) and c) 72h (enlarged sheet).

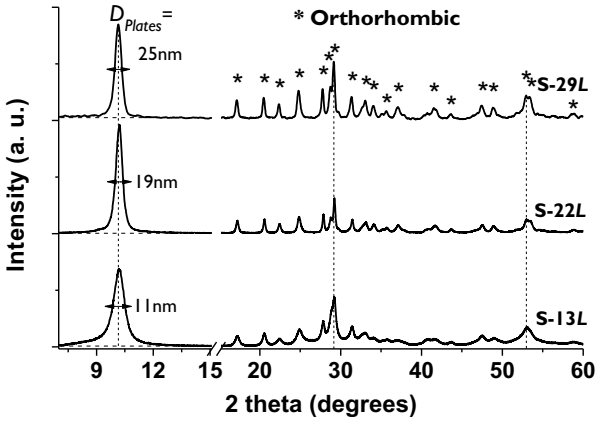

A)

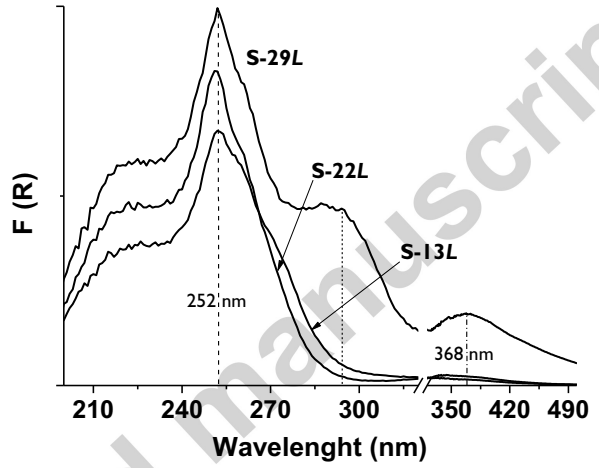

B)

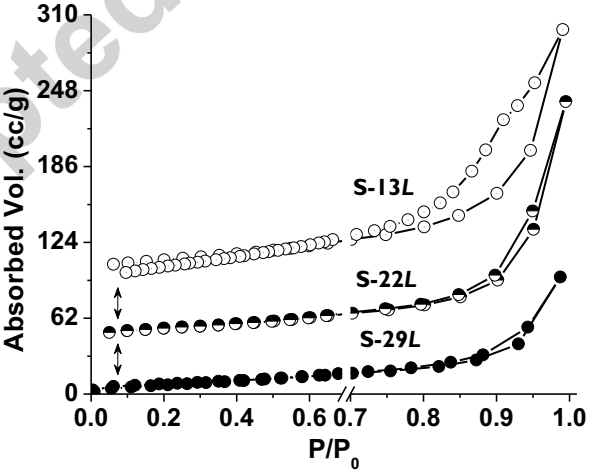

C)

Figure 2. A) X-ray diffraction patterns, B) UV-Vis diffuse reflectance spectra and C) N_2 adsorption-desorption isotherms for the $ZnS(en)_{0.5}$ hybrid semiconductors prepared at different aging times; 6h (S-13*L*), 48h (S-22*L*) and 72h (S-29*L*).

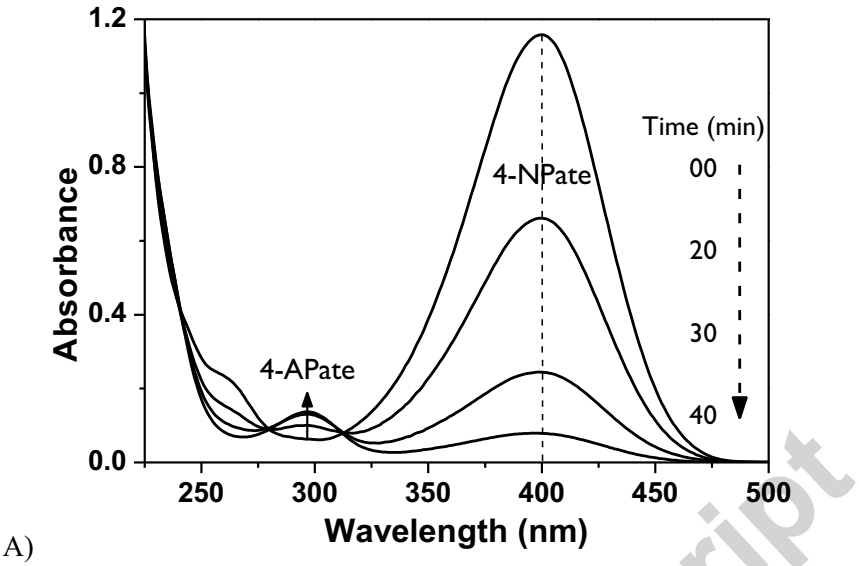

A)

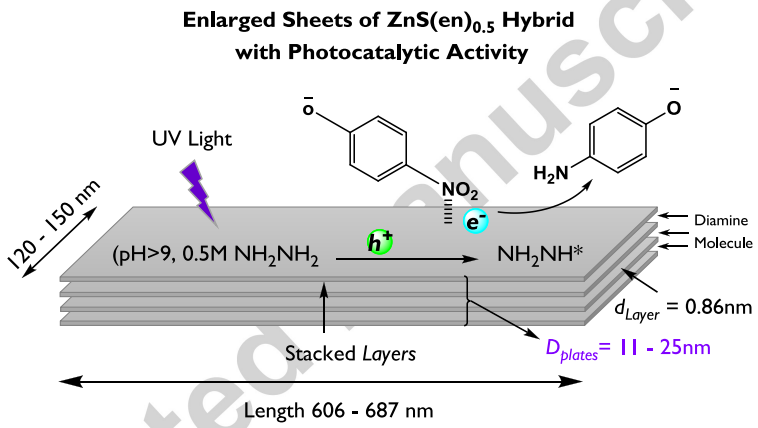

B)

Figure 3. A) UV-Vis spectra, B) Schematic representation of the mechanism of the photoconversion of *4-nitrophenol* to *4-aminophenol* in the presence of hydrazine over the stacked layer structure of the enlarged sheets of ZnS(*en*)$_{0.5}$ hybrid semiconductor.